Electronic Supplementary Information (ESI)

3D micro-porous conducting carbon beehive by single step polymer carbonization for high performance supercapacitor: The magic of *in situ* porogen formation

Dhanya Puthusseri[a], Aravindan Vanchiappan[b], Madhavi Srinivasan[b] and Satishchandra Ogale[a*]

[a] *Centre of Excellence in Solar Energy, Physical and Materials Chemistry Division, National Chemical Laboratory (CSIR-NCL), Pune 411 008, India; Network Institute of Solar Energy (CSIR-NISE), New Delhi, India*
Fax: +91 20 2590 2636, E-mail: sb.ogale@ncl.res.in
[b] *Division of Materials Science , Nanyang Technological University*
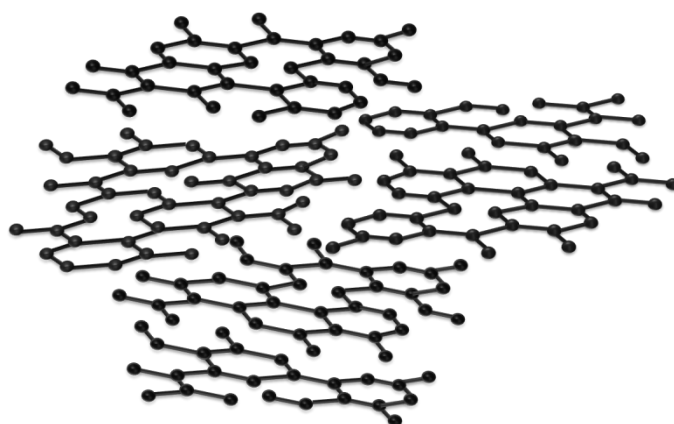Singapore 639798

1

ESI-I

Figure SI-1. Schematic representation of turbostratic carbon
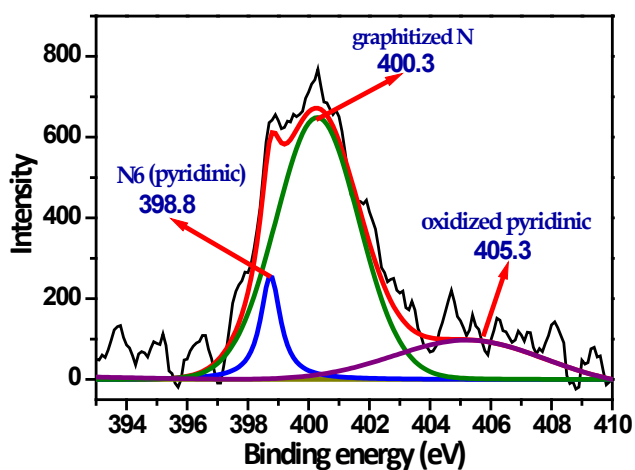

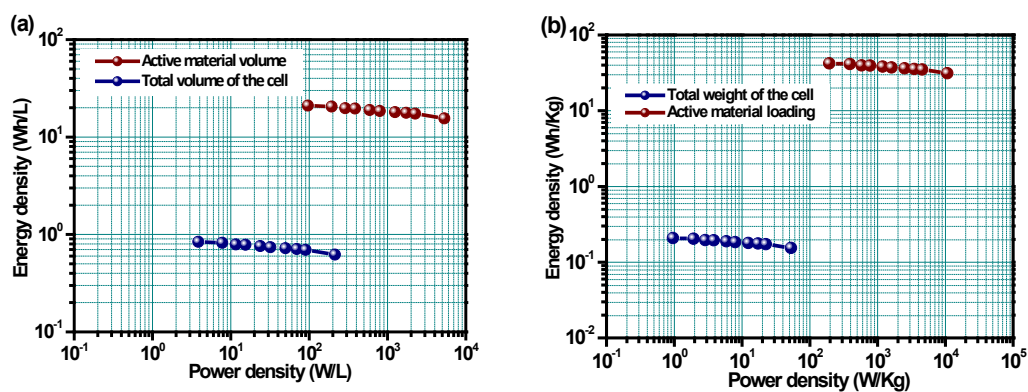*Figure SI-2. N1s XPS spectrum of IMPC*

Figure SI-3. Ragone plot of (a) volumetric energy density and power density based on active material volume and the cell volume; and (b) gravimetric energy density and power density based on total active material loading and total weight of the cell

Polymer used	Surface area (m^2/g)	
	w/o activation	After activation
Poly (4-sodium styrene sulfonate-co-maleic acid) sodium salt[1]	1720	-
Copolymer of polyacrylonitrile (PAN), and poly(n-butyl acrylate) (PBA)[2]	500	2570
Polypyrole[3]	-	3432
Poly(acrylic acid-co-maleic acid) sodium salt[4]	188	-
Poly(o -phenylenediamine)[5]	-	591
Sulfonated Poly(styrene-co-methacrylic acid) (SPS-COOH) Sphere[6]	508	
Polypyrole[7]	-	2870
Poly(acrylamide-*co*-acrylic acid) potassium salt	**1327**	**2366**

Table SI-1. Specific surface area of carbons obtained by the pyrolysis of polymer

.

References

1.   P. Yadav, A. Banerjee, S. Unni, J. Jog, S. Kurungot and S. Ogale, *ChemSusChem*, 2012, **5**, 2159-2164.
2.   M. Zhong, E. K. Kim, J. P. McGann, S.-E. Chun, J. F. Whitacre, M. Jaroniec, K. Matyjaszewski and T. Kowalewski, *Journal of the American Chemical Society*, 2012, **134**, 14846-14857.
3.   L. Wei, M. Sevilla, A. B. Fuertes, R. Mokaya and G. Yushin, *Advanced Functional Materials*, 2012, **22**, 827-834.
4.   P. Yadav, S. Warule, J. Jog and S. Ogale, *Solid State Communications*, 2012, **152**, 2092-2095.
5.   H. Zhu, X. L. Wang, X. X. Liu and X. R. Yang, *Advanced Materials*, 2012, **24**, 6524-6529.
6.   J.-S. Lee, S.-I. Kim, J.-C. Yoon and J.-H. Jang, *ACS Nano*, 2013.
7.   L. Qie, W. Chen, H. Xu, X. Xiong, Y. Jiang, F. Zou, X. Hu, Y. Xin, Z. Zhang and Y. Huang, *Energy & Environmental Science*, 2013, **6**, 2497-2504.

ESI-II

We also examined the effect of adding an activation agent (KOH) to the polymer (ratio 1:1 wt.%) before pyrolysis to enhance the surface area and possibly the capacitance. The carbon sample thus obtained is named as IMPC-A. The BET specific surface area obtained from N_2 gas adsorption desorption studies on this sample was 2366 m^2/g which is significantly higher than that (1327 m^2/g) for IMPC (i.e. carbon obtained without KOH addition). The N_2 adsorption desorption isotherms and pore size distributions for IMPC and IMPC-A are shown in the Figure. SII-1.
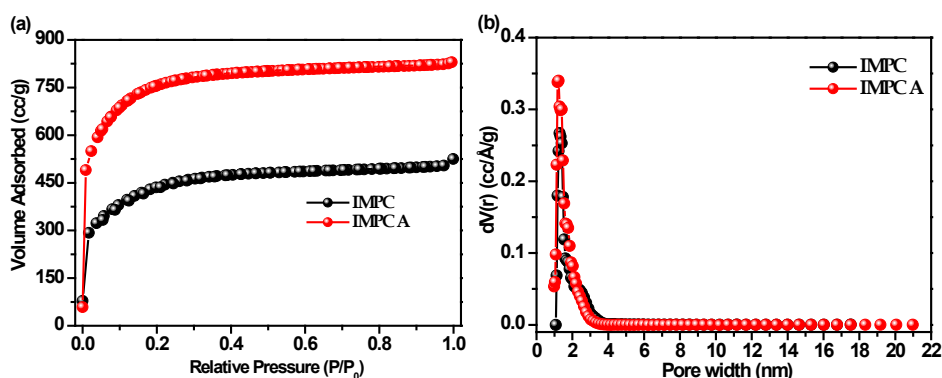

Figure SII-1. (a) Isotherm and (b) pore size distribution of IMPC and IMPC Activated (IMPC A)

From the pore size distribution curve it is clear that the density of micropores is enhanced after activation, but there are no other discernible modifications. The electrochemical performance of IMPC-A in 1M H_2SO_4 was studied using galvanostatic charge discharge measurement at various current densities. The galvanostatic charge-discharge and variation of capacitance with current density are shown in Figure. SII-2.
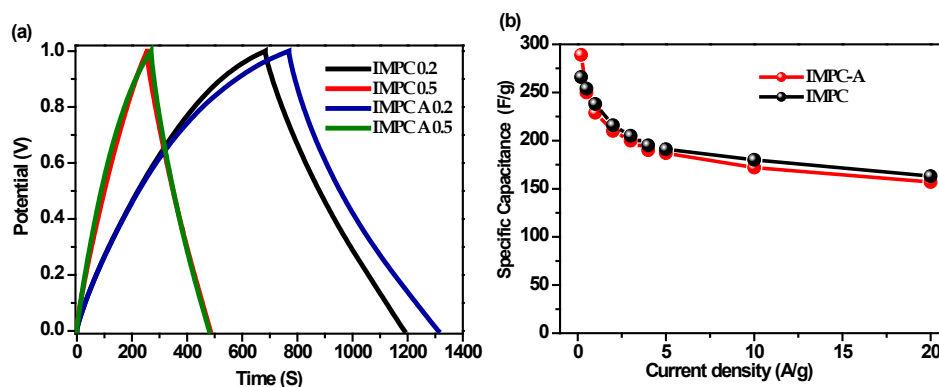

Figure SII-2 (a) Galvanostatic charge discharge at low current densities and (b) Specific capacitance calculated form charge discharge of IMPC and IMPC Activated (IMPC A).

4

IMPC-A showed an enhancement in the specific capacitance at lower discharge rate whereas it did not show increase in specific capacitance at higher current densities. This may be due to the fact that IMPC-A has higher micropore density than that of IMPC whereas the ratio of mesopores to micropores is higher for IMPC. Thus at low charging rates more inner pores will be accessible for the solvated electrolyte ions, yielding higher capacitance. But at higher current densities, due to less mesopore density and large diffusion length, the accessible surface area for electrolyte ions is less as compared to the case of lower current density. Increase in the resistance due to increased defects and oxygen content after activation is also a hindrance to the capacitance enhancement. The XPS spectra of IMPC-A is shown in the Figure.SII-3 and the percentage of elements is listed in Table SII-1. It is clear that the oxygen content has increased after activation.
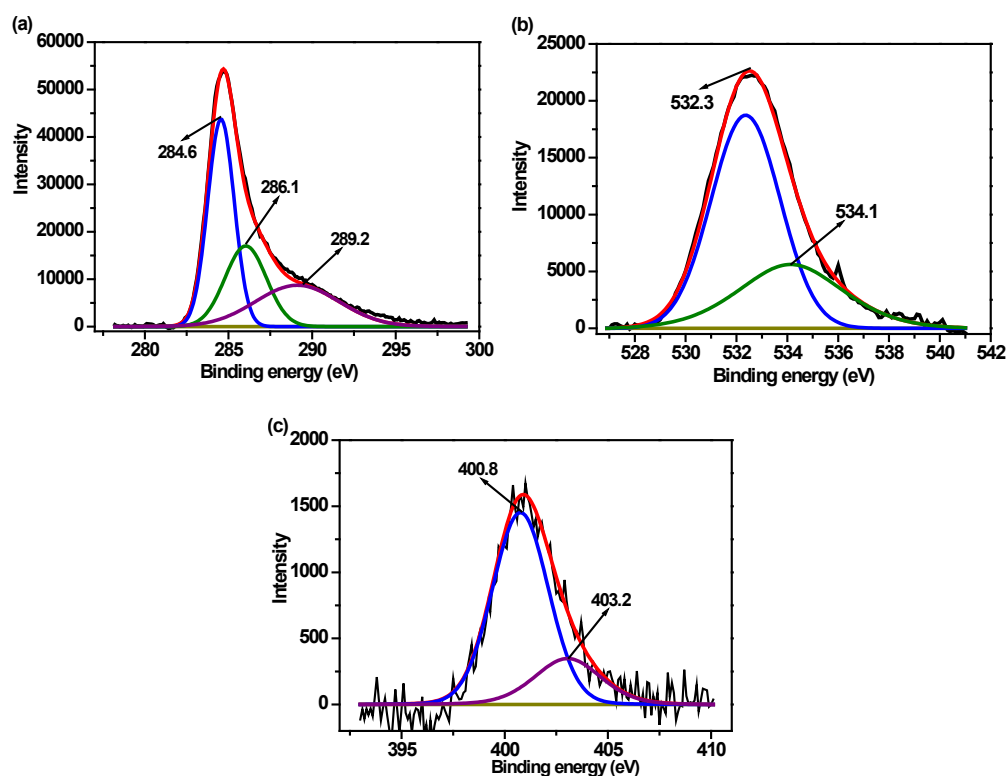

Figure. SII-3. (a) C1s, (b) O1s and (c) N1s XPS spectra of IMPC A

	C %	N %	O %	Surface area (m^2/g)
IMPC	89.2	1.9	9.9	1327
IMPC A	83.3	1.6	15.1	2366

Table SII-1. Amount of different elements and specific surface area of IMPC and IMPC A